Thylacinus (Marsupialia: Thylacinidae) from the Mio-Pliocene boundary and the diversity of Late Neogene thylacinids in Australia.

Adam Yates

Thylacinus yorkellus is described as a new, moderately small-bodied species of thylacinid from the latest Miocene or, more likely, earliest Pliocene of South Australia. The new species can be diagnosed by the autapomorphic presence a strongly developed precingulid that terminates in a cuspidule on the anterobuccal face of the paraconid of the lower molars and a tiny basal anterior cuspidule on P₂, P₃ and the lower molars. It is found by cladistic analysis to be the sister species of the recently extinct *Th. cynocephalus* and distinct from the approximately coeval *Th. megiriani* from the Northern Territory. New dentary material is described and referred to *Th. megiriani*. These add character data and allow this species to be re-diagnosed based on autapomorphic character traits. Each of the three known Late Miocene to Early Pliocene *Thylacinus* species (*Th. potens, Th. megiriani* and *Th. yorkellus*) suggest that, instead of declining, there was a modest radiation of *Thylacinus* in the Late Miocene.

- 2 Adam M. Yates
- 3 Museums and Art Galleries of the Northern Territory
- 4 Museum of Central Australia, P.O. Box 831, Alice Springs, Northern Territory, 0871
- 5 Australia
- 6 Corresponding author: Adam M. Yates, Museum of Central Australia, P.O. Box 831, Alice
- 7 Springs, Northern Territory, 0871, Australia, ph. +61 (08) 89511148, email:
- 8 adamm.yates@nt.gov.au

9

Introduction

- The tragic tale of hylacinidae, or the marsupial wolves, involves a sustained loss of diversity from an early to middle Miocene high (Wroe 203) up to the final extermination of the last surviving population of *Thylacinus* 12
- 13
- cynocephalus at our own harmin the early twentieth century (Thornback and Jenkins, 1982; Fisher and 14
- 15 Blomberg, 2011). Just when the Thylacinidae became restricted to a single species is an interesting question
- 16 that might relate to broadscale changes in Australian terrestrial ecosystems during the latter part of the
- 17 Cenozoic. It has been noted that the late Miocene diversity of thylacinids is severely depleted (Rich, 1991;
- 18 Wroe and Muirhead, 1999; Wroe, 2003), although the dearth of fossil deposits from this time is a confounding
- 19 factor. Nevertheless has one popular account suggested that the wolf-sized *Th. potens* from the Alcoota Local
- 20 Fauna (Woodburne, 1967) was the sole surviving lineage by this time and that it was directly ancestral to the
- 21 modern Th. cynocephalus (Archer, Hand and Godthelp, 1991).
- Subsequently *Tyarrpecinus rothi*, a small plesiomorphic thylacinid that apparently lay outside the genus 22
- 23 Thylacinus, was discovered in the Alcoota local fauna demonstrating that at least two thylacinid lineages were
- 24 surviving at this point in the Late Miocene (Murray and Megirian, 2000). However all thylacinids from younger
- 25 local faunas belong to Thylacinus, indicating that Ty. rothi was a late surviving relict that probably died out
- 26 shortly after the deposition of the Alcoota Local Fauna. The discovery of Ty. rothi does not falsify the
- 27 hypothesis that Th. potens was part of a single anagenetic lineage of large-bodied thylacinids that led directly
- 28 to Th. cynocephalus. Therefore the scenario where Thylacinidae was reduced to a single lineage prior to the
- 29 close of the Miocene remained a viable hypothesis.
- 30 A further large-bodied Thylacinus species, Th. megiriani, was discovered in the Ongeva Local Fauna which
- 31 derives from a channel-fill in the Waite formation that overlies the Alcoota Local Fauna on Alcoota Station
- 32 (Murray, 1997). The Ongeva Local Fauna correlates with the Beaumaris Local Fauna from the Black Rock
- 33 Sandstone in the Port Philip Basin of south-eastern Australia based on the shared presence of Zygomaturus qilli
- 34 (Megirian, Murray and Wells, 1996; Murray, 1997; Megirian et al., 2010). The Black Rock sandstone also
- 35 preserves a marine invertebrate fauna and has a robustly stratigraphically controlled age of 6.2-5.0 ma, an age
- 36 that straddles the Mio-Pliocene boundary (Dickinson et al., 2002). Th. megiriani shares more derived features
- 37 with the modern Th. cynocephalus than with Th. potens. Thus Th. megiriani could be interpreted as
- chronospecies on an anagenetic lineage leading from *Th. potens* to *Th. cynocephalus*. 38
- description Th. megiriani was known only from its holotype which is a single broken niaxila with worn and 39
- 40 damaged teeth. However a couple of large thylacinid dentary fragments have been found in the Ongeva Local
- 41 Fauna since the initial publication that can be referred to this species. Character data from these specimens
- 42 has been incorporated into a phylogenetic analysis of thylacinid relationships (Yates, 2014) but they have not
- 43 been described or adequately illustrated in the scientific literature.
- 44 There is a further thylacinid from the penecontemporaneous Curramulka Local Fauna of South Australia
- 45 (Pledge, 1992) that sheds light on the number of thylacinid lineages present in Australia during the latest
- 46 Miocene and earliest Pliocene. This thylacinid is described here as a new species. In addition the new
- 47 mandibular specimens of Th. megiriani are described and the species diagnosed with autapomorphic
- 48 characters. This new data casts strong doubt on the hypothesis of a single anagenetic lineage of Thylacinus in
- 49 the late Neogene of Australia.

Systematic Palaeontology

51

50

- 52 Dasyuromorphia Gill, 1872
- 53 Thylacinidae Bonaparte, 1838
- 54 Thylacinus Temminck, 1824
- 55 Thylacinus yorkellus sp. nov.
- 56 urn:lsid:zoobank.org:act:D176F98E-740B-4E37-A491-3AFDCCC1CD50
- 57 Holotype. South Australian Museum (hereafter SAM) P29807, incomplete left dentary with C, P₁₋₃ and M₂₋₃ (Fig.
- 58 1-2, Table 1-2).
- 59 Referred specimen. SAM P38799, crown of right M₃ (Fig. 3-4, Table 2).
- 60 Locality and stratigraphic age. Corra-Lynn Cave, approximately 3km south of Curramulka, York Peninsula,
- 61 South Australia. Late Miocene or, more likely, early Pliocene in age.
- 62 Etymology. From York Peninsula and the diminutive suffix –ellus (Latin), referring to its small size relative to Th.
- 63 cynocephalus.
- 64 Diagr Differs from all thylacinids by the presence of the following autapomorphies: Lower molars with a
- 65 strongly developed precingulid that terminates in a cuspidule on the anterobuccal factorial the paraconid and a
- tiny basal anterior cuspidule on P₂, P₃ and the lower molars. It can be further distinguished from *Th. macknessi*
- and all thylacinids not in the genus *Thylacinus* by the complete absence of metaconids on M₂, M₃ and,
- presumably, M₄. It can be further distinguished from *Th. potens* by its smaller size (estimated adult body mass
- of 16-18 kg vs. 39-56 kg for Th. potens; Yates, 2014), by the presence of wide diastemata between each of the
- lower premolars as well between P₃ and M₁, and by the presence of deep cleft-like carnassial notches on the
- 71 lower molars. It can be further distinguished from *Th. megiriani* by its smaller size (estimated body mass of *Th.*
- 72 megiriani is 57 kg; Wroe, 2001), wider diastemata separating P₃ from M₁ and P₂ from P₃ its relatively gracile and
- 53 buccolingually compressed anterior dentary lacking a ventrolateral torus, the complete absence of any trace of
- the metaconid on the lower molars, and by the presence of deep cleft-like carnassial notches on the lower
- 75 molars. Lastly it can be further distinguished from Th. cynocephalus by the lengths of both P_2 and P_3 exceeding
- 76 that of M_1 and the sense of a diastema between the canine and P_1 .
- 77 Remarks. Pledge (1992) figured and briefly descript the holotype specimen in his description of the
- 78 Curramulka Local Fauna. He suggested that it may belong to an undescribed species but declined to name it.
- 79 With our improved knowledge of thylacinid diversity and the addition of a second specimen showing the same
- 80 autapomorphic characters of the molars as the holotype, there is now sufficient evidence to warrant the
- 81 naming of a new species.

Description

- 84 The holotype includes the incisor alveoli, the canine, all three premolars, M_2 , M_3 and the alveolus for M_1 (Fig. 1-
- 85 2, Table 1-2). Posteriorly the dentary has broken off at the level of the posterior end of M_3 , so that M_4 is
- missing. The dentary is transversely compressed, as it is in Th. cynocephalus but unlike the transversely broad, 86
- robust dentaries of Th. megiriani and some Th. potens. If fers further from Th. megiriani and Th. potens in 87
- 88 lacking a thickened torus along the ventrolateral margin, below the mental foramina. The dentary depth below
- 89 the anterior root of M₂ (the posteriormost level at which this measurement can be made) is 24.5 mm which
- 90 lies within the range of Th. cynocephalus. Given that the length of the lower-olar row and the heights of the
- individual molars lie below the range seen in *Th. cynocephalus*, it would sethat the holotype *Th. yorkellus* 91
- 92 has a deeper jaw relative to tooth size in comparison to the former species. A relatively deep dentary is also
- 93 seen in some, but not all, specimens of Th. potens (Yates, 2014). The lateral surface of the dentary is pierced by
- 94 three mental foramina set approximately at the mid height of the dentary, although it is possible that a fourth
- 95 was present in what is now a large area of missing bone below P₃ (Fig. 2). The anterior mental foramen is large
- 96 anteriorly facing opening with a diameter of 3.2 mm located below the anterior root of P₂. The two close-set
- 97 posterior mental foramina are placed below M₂ and the anterior margin of M₃, respectively. These openings
- 98 are smaller, with anteroposterior diameters of 2.1 and 1.4 mm, respectively. In lateral view the alveolar margin
- 99 is concave with P₃ set lower than the rest of the preserved tooth row. The medial symphyseal surface extends
- 100 posteriorly to the level of the anterior margin of P₃.
- 101 The canine has a procumbent root and a vertically projecting crown. The tip is gently recurved so that the
- 102 mesial margin in lateral view is convex and the distal margin is concave. In anterior view the crown has a weak
- 103 lingual curvature. The cross-section of the crown is a slightly bucco-lingually compressed oval. A weakly
- 104 developed carina extends along the anterolingual margin of the crown, from base to apex. The distal surface is
- 105 rounded and smooth. The measurements of the canine are given in table 1.
- 106 A diastema of 3.3 mm separates the canine alveolus from that of P_1 . P_1 is a small, low-crowned tooth. In
- 107 occlusal view is elongately ovoid with the long axis oriented anteroposteriorly, Although the tip of the
- 108 protoconid is well worn, it is clear that the unworn tooth would have had a height less than its anterior-
- 109 posterior length. The apex of the protocone is located in the anterior half with an elongate heel extending
- 110 posterior to it. The heel has a sharp posterior corner which forms an incipient cuspidule. In lateral view the
- 111 distal margin of the protoconid curves gently down to the distal heel. A weakly developed cristid extends along
- 112 the mesial margin of the protoconid. The tooth has no other cristids or cuspidules.
- A diastema of 2.8 mppparates P₁ from P₂. P₂ differs from P₁ in being larger (Table 2) and proportionately 113
- 114 taller. The apex of large, triangular protoconid is less skewed to the mesial side of the tooth, being placed
- 115 slightly mesial to the mid length. A weak cristid extend up the mesial side of the protoconid. There is a minute
- 116 tubercle-like cuspidule developed at the base of this mesial cristid. A distal cristid extends from the apex of the
- 117 protoconid to the distal corner of the basal heel. A distinct inflection in the lateral profile marks the change
- 118 from the heel to the distal margin of the protoconid.
- 119 A long diastema of 6.4 mm sepparates P₂ from P₃. P₃ is larger than, P₂ and differs from it in a number of subtle
- 120 features. P₃ shows a greater development of the mesial basal cuspidule than in P₂. The large protoconid is

centrally located and triangular in lateral view, the medial and distal margins bear cristids. In occlusal view the crown is widest distally, where the heel now rems an incipient talonid basing shallow notch in the lateral profile now separates the distal heel from the protoconid, and the distal heel new orms a protrusive cuspidule 121 122 123 124 with a worn tip. 125 M₁ is missing, and the lingual alveolar margin of the dentary is missing from the level of the distal root of P₃, 126 posteriorly. Nevertheless the buccal side of the M_1 alveolus is separated from P_3 by a diastema of 3.0 mm, 127 whereas there is no diastema between the alveolus of M_1 and M_2 . 128 M₂ consists of two large trigonid cusps (paraconid and protoconid) and three far smaller cusps (hypoconid, 129 hypoconulid and entoconid) surrounding the talonid basin. The most remarkable feature of M2 (and M3) is the 130 strength of the short precingulid, which forms a sharp-edged shelf that terminates in a well-developed 131 cuspidule on the anterobuccal face of the base of the paraconid. The precingulid slopes steeply distaloyed ally 132 from this cuspidule and terminates near the base of the crown level with the mesial margin of the protoconid. 133 The paraconid is well developed and triangular in occlusal view. A minute cuspidule is developed on the 134 anterior slope of the paraconid, near the base of the crown, at about the same level as the anterobuccal 135 cuspidule of the precingulid. The protoconid forms the largest cusp of M₂. In lateral view the mesial margin of 136 the protoconid curves distally towards the apex, however this shape has been created by wear. A distinct, tear-137 drop shaped wear facet is developed at the tip of the protoconid and extending down its anterior side, along 138 the course of the paracristid. A deep carnassial notch is developed between the paraconid and protoconid, 139 dividing the paracristid into two sections. There is no trace of a protocristid or a metaconid on the posterior 140 side of the protoconid, although the cristid obliqua extends approximately half way up this surface. The cristid 141 obliqua is also divided into two sections by a deep carnassial notch, this time separating the protoconid from 142 the hypoconid. In buccal and lingual view the talonid is set distinctly lower than the trigonid. In occlusal view its 143 transverse width is slightly greater than that of the trigonid. All of the cusps of the talonid are highly worn and 144 flat-topped. The largest of these and the most strongly projecting is the buccally placed hypoconid. The 145 posteriorly located hypoconulid has been virtually obliterated by wear and is only recognisable as a slight 146 thickening of the enamel around the posterior rim of the wear facet. The very small entoconid is placed on the 147 lingual side of the talonid, slightly inset from the lingual margin of the crown. A short ridge extends 148 posterobuccally from its apex towards the hypoconulid. A short postcingulid extends obliquely up the posterior 149 surface of the hypoconid from a basally located point on the buccal side to a more apical point on the lingual 150 side. M₃ is very much the M₂, differing in the following respects. The minute anterior cuspidule at the base of the 151 paraconid is every ss well-developed. The protoconid is taller, and the cristid obliqua extends for less than half 152 153 its height up the posterior surface. The talonid is slightly narrower than the trigonid and the hypoconulid forms 154 a low conical cuspid. The posterobuccal ridge extending from the apex of the entoconid joins the anterior base 155 of the hypoconulid, thus creating a small oval basin that is separated from the main talonid basin. A low but 156 sharp postcristid between the hypoconulid and the entoconid forms the posterolingual margin of this small 157 oval basin. The postcingulid is very reduced, and is little more than a shallow depression on the posterior

158

surface of the hypoconid.

- 159 The M₃ of SAM P38799 shows some minor differences from the holotype but the main features are the same,
- 160 including the distinctive precingulid terminating in an anterobuccal cuspidule (Fig. 3-4, Table 2). In this
- 161 specimen the anterior cuspidule at the base of the paraconid is better developed than in either of the two
- molars of the holotype, and has an incipient preparacristid leading from it towards the apex of the paraconid.
- 163 The talonid is as wide as the trigonid and the entoconid appears to lack the posterobuccal ridge that links it to
- the hypoconulid.

Size estimate

- 166 Calculating from the third lower molar length regression formula, derived from the dasyuromorphian-only data
- set of Myers (2001), a body mass estimate of 17.8 kg is obtained for the holotype and 15.9 kg for SAM P38799.
- 168 These estimates are well below the average body mass of 29.5 kg for recent Tasmanian *Th. cynocephalus*
- (Paddle, 2000) but are not outside the range estimated for mainland Holocene samples of this species (Letnic,
- 170 Fillios and Crowther, 2012). However, it is clear that *Th. yorkellus* was a far smaller species than either *Th.*
- 171 potens or Th. megiriani which have estimated body masses ranging between 38.7 and 57.3 kg (Wroe, 2001;
- 172 Yates, 2014).
- 173 Thylacinus megiriani Murray, 1997
- 174 Holotype. NTM P9618, fragmentary left maxilla with P¹⁻³ and M¹⁻³
- 175 Referred specimens. NTM P4376, anterior fragment of a right dentary containing the alveoli with broken roots
- 176 for P₂, P₃ and M₁ and the empty alveolus for M₂ (Fig. 5-7). NTM P4377, posterior fragment of a right dentary
- 177 containing an incomplete M_4 (Fig. 8-10).
- 178 Locality and stratigraphic age. 'South Quarry', an excavation on the south-western side of 'Hill 1' (Woodburne
- 179 1967) an erosional remnant of the upper Waite Formation on the Alcoota Fossil Reserve. Ongeva Local Fauna,
- 180 latest Miocene or earliest Pliocene in age.
- Diagros. Differs from all thylacinids by the presence of the following autapomorphies: a short, lobe-like
- 182 postcingulum between the metastyle and protocone of M²; hypertrophied ventrolateral torus of the dentary
- 183 with the buccolingual width of the dentary at the level of P₃ that is greater than 75% its depth at the same
- 184 level. The presence of a small stylar cusp E on M² and M³ might also be an autapomorphic reversal within the
- 185 genus Thylacinus but the optimisation of the character is ambiguous due to its presence in the closely related
- outgroup, Wabulacinus ridei, and the absence of a preserved M² or M³ for Th. macknessi. Similarly the
- 187 presence of a vestigial metaconid and metacristid on M_4 (and presumably the other lower molars) is
- ambiguous due to the presence of metaconids in *Th. macknessi* and their absence in *Th. potens*. This may
- 189 represent an autapomorphic reversal in *Th. megiriani* or a case of convergent loss in *Th. potens* and the *Th.*
- 190 yorkellus + Th. cynocephalus clade. It can be further distinguished from Th. macknessi and all non-Thylacinus
- thylacinids by: its greater size; the great reduction of the size of the paracone relative to the metacone;
- 192 elongation of the postmetacrista, so that it is greater than 52% the length of the tooth in M² and M³. It can be
- 193 further distinguished from *Th. potens* by: the long axis of P¹ aligned with those of the other upper premolars;
- the length of M¹ is greater than its width; the complete absence of a precingulum on M¹ and M³; the absence

195 of a metaconule on all upper molars; M3 much longer (>5%) than M2; M3 longer than wide; presence of a 196 diastema between P₃ and M₁. 197 Remarks. The new dentary specimens cannot be referred to Th. megiriani on the basis of autapomorphic 198 characteristics due to their fragmentary nature and lack of overlap with the holotype maxilla. However the 199 apparent reversal to the presence of an, albeit vestigial, metaconid parallels the reappearance of a tiny tubercular stylar cusp the upper molars of the holotype. 200 Furthermore they erive from the same level in the same quarry as the holotype, are of an appropriately large 201 202 size, and can be distinguished from Th. potens, which is the only other large-bodied thylacinid known from a 203 similar time and place. For these reasons it is reasonable to refer them to Th. megiriani. 204 Description of the new mater 205 206 The anterior dentary fragment (NTM P4376; Fig. 5-7, Table 3) has only broken roots and empty alveoli and 207 does not contain any tooth crowns. This coupled with poor preservation means that it is not immediately 208 obvious exactly which teeth the roots and alveoli belong to and therefore the disposition of the teeth in the 209 jaw. However several lines of evidence indicate that the posterior two empty alveoli are for the anterior and 210 posterior roots of M₂, respectively, while the posterior two projecting root stumps are the mesial and distal 211 roots of M₁. Anterior to the molar alveoli there are the broken roots and alveoli of P₂ and P₃ (Fig. 7). Evidence 212 for this interpretation comes from a partial bridge of finished bone between the second and third preserved 213 alveoli, indicating that there was a diastema between two different teeth in this position, rather than these 214 alveoli representing the anterior and posterior alveoli of the same tooth. The posterior limit of medial 215 symphyseal surface is level with the front margin of the fourth alveolus. As the posterior end of the symphysis 216 draws level with P₃, or at least the diastema between P₂ and P₃ in all thylacinid specimens examined, the third 217 and fourth alveoli in NTM P4376 should represent the anterior and posterior alveoli for P₃. From the alveoli it 218 can be seen that there was no diastema between M_1 and M_2 , but there was a short diastema of 3.6 mm 219 between P₃ and M₁, and a slightly longer diastema of 4.0 mm between P₂ and P₃. 220 The dentary is dorsoventrally shallow but mediolaterally thickened, giving it a distinctly robust appearance. 221 Adding to the thickness of the jaw is a strong torus developed along the ventrolateral margin of the dentary 222 from a point level with the midlength of P₂ to one level with the distal end of M₁. At the maximum thickness of 223 the torus (level with the posterior root of P_3) the dentary measures 20.8 mm wide, which approaches the 224 dorsoventral depth of the dentary at the same level (27.0 mm). The lateral surface of the dentary, above the 225 ventrolateral torus, is pierced by three mental foramina. The anterior-most mental foramen lies anterior to the 226 alveoli for P2, the middle foramen lies level with the anterior end of P3, and the posterior foramen lies level 227 with the posterior end of M₁. 228 The second specimen (NTM P4377; Fig. 8-10, Table 4) is a small fragment from the posterior end of a right 229 dentary including a partial M₄ and the anterior base of the coronoid process. The medial surface of the dentary

is gently convex dorsoventrally, whereas the lateral surface bears a ridge that slopes posterodorsally to merge

with the leading margin of the coronoid process. The lateral ridge forms the lower border of a flat

230

232 dorsomedially facing surface that occurs below the fourth lower molar. The ventral part of the dentary is 233 missing so the depth to height ratio cannot be measured. The incomplete M₄ includes the talonid and the 234 posterior side of the protoconid. The protoconid is tall with an almost vertically oriented posterior margin. The 235 protocristid extends from the apical tip of protoconid to a small tubercle about half-way down the posterior 236 face of the protoconid (Fig. 10). This tiny tubercle appears to be a vestigial remnant of the metaconid which is 237 usually absent in derived species of Thylacinus. Two weakly developed cristids extend ventrally from the 238 tubercle. The two cristids diverge at a highly acute angle. The more buccally placed cristid is the cristid obliqua. 239 It extends to the base of the protoconid and up the anterior face of the hypoconid. A shallow, weakly 240 developed carnassial notch is created between the hypoconid and the protoconid. This notch is similar to the 241 weak notches developed on the lower molars of Th. potens and unlike the deep clefts that can be observed in 242 the carnassial notches of the lower molars of Th. yorkellus and Th. cynocephalus. The lingual cristid that 243 branches from the tubercle on the posterior face of the protoconid is interpreted as a metacristid. It 244 terminates at the base of the protoconid without extending onto the talonid. Its presence strengthens the 245 interpretation of the tubercle as a vestigial metaconid. The moderately large, conical hypoconid comprises the 246 talonid which bears no other cusps. The anterobuccal face of the hypoconid is planed off by an oblique wear 247 facet that faces buccodorsally. The weak cristid obliqua extends directly anteriorly from the apex of the 248 hypoconid. The anterolingual rim of the hypoconid is rounded, lacking a postcristid.

Cladistic Analysis

- 250 Th. yorkellus was included in an earlier cladistic analysis of thylacinid relationships (Yates 20 This analysis
- already included data from the mandibular specimens of *Th. megiriani* described in this paper. The same
- characters from the previous were employed with one magnetic ation to character 36. Previously this character
- 253 simply described the absence (0) or presence (1) of carnassial notch in the cristid obliqua of the lower molars.
- 254 In the present analysis the derived state is divided into two states: a weakly-developed shallow carnassial
- 255 notch (1) or a deep, strongly-developed carnassial notch (2). The multistate character is treated as ordered.
- 256 The score for character 34 (metaconid size in m₂₋₄) of Thylacinus megiriani was changed from 2 (completely
- absent) to 1 (present as a minute cuspidule) in the light of the new evidence presented above.
- 258 The resulting matrix (Appendix 1) was subjected to a maximum parsimony analysis in PAUP 4.0b (Swofford,
- 259 2002) using the following settings: heuristic search; random addition sequence with 500 replicates; and TBR
- 260 branch-swapping algorithm. The strength of the internal nodes was tested with a bootstrap analysis (1000
- 261 bootstrap replicates, heuristic searching with 50 addition sequence replicates).
- 262 The search resulted in two equally most parsimonious trees of 93 steps. The topologies of these two trees are
- completely congruent with the two trees obtained in the earlier analysis (Yates, 2014) with the loss of
- resolution entirely the result of a variable position of *Maximucinus muirheadae*. If this wildcard taxon is pruned
- 265 a posteriori a fully resolved tree is obtained (fig. 11a). Th. yorkellus is found to be the sister species of the
- 266 modern *Th. cynocephalus*. The *Th. yorkellus* + *Th. cynocephalus* is relatively robust with the second highest
- bootstrap score of all the internal clades (71 %, fig. 11b). Nevertheless missing data reduces the number of
- unambiguous apomorphies of this clade to one: the presence of a deep, well-developed carnassial notch
- cristid obliqua on each of the lower molars.

270 271 Disscussion 272 The recognition of Th. yorkellus increases the number of Thylacinus species in the Late Miocene - Earliest 273 Pliocene interval to three: Th. potens, Th. megiriani and Th. yorkellus. A fourth lineage, that of the recent Th. 274 cynocephalus, can also be inferred to have arisen in this period (Fig. 12). None of the local fauna that produced 275 the three known species can be directly dated but they do appear to form a stratigraphic sequence. The 276 Ongeva Local Fauna occurs in a channel incised into sediments that overlie those that contain the Alcoota Local 277 Fauna, directly demonstrating that the former is younger than the latter (Megirian, Murray and Wells, 1996). 278 However the absolute age difference between them is probably not great because many species are shared 279 between the two deposits including the biostratigraphically important Kolopsis torus (Megirian, Murray and 280 Wells, 1996). The presence of Zygomaturus gilli in the Ongeva Local Fauna indicates that it may be correlated 281 with the Beaumaris Local Fauna from the Black Rock Sandstone of Port Phillip Bay (Megirian, Murray and 282 Wells, 1996). The Beamaris Local Fauna straddles the Mio-Pliocene boundary on the basis of local strationphic 283 controls and its included marine invertebrate fauna (Dickinson et al, 2002). The relative difference between the 284 Ongeva Local Fauna and the Curramulka Local Fauna is difficult to determine. Pledge estimated that the 285 deposit was late Miocene in age which would make it roughly contemporaneous with, or possibly older than 286 the Ongeva Local Fauna. However a constrained seriation analysis clustered the Curramulka Local Fauna with 287 younger Pliocene local faurka, that were given the age-name Tirarian while the Ongeva Local Fauna was 288 clustered with the Beaumaris and Alcoota Local Fauna in the Waitean Age (Megirian et al. 2010). A younger 289 age for the Curramulka Local Fauna is supported by the presence of a number of macropodid genera that are 290 not known from the older Waitean fauna, including: Baringa, Troposodon and Protemnodon (Pledge, 1992). 291 Nevertheless the Curramulka Local Fauna is probably one of the oldest Tirarian assemblages due to its total 292 lack of rodent remains, despite intensive fine sieving of the silty matrix and presence of numerous other small 293 vertebrates (Pledge, 1992). Thus an early Pliocene age of 4.5 ma or older would appear likely based on the timing of the appearance of rodents in other fossil deposits in Australia (Breed and Ford, 2007) 294

These three deposits depen to form a stratigraphic and the sequence matches the branching 295 order of *Thylacinus* species recovered in the cladistic alysis, supporting the hypothesis of an anagentic 296 297 lineage. However, the time difference ween them is probably too small for a plausible anagenetic sequence. 298 It is quite likely that all three local faultaspan no more than 2 or 3 ma, from 5 ma to 7 or 8 Ma. If *Th. potens*, 299 Th. megiriani and Th. yorkellus did indeed form an anagenetic lineage then the turnover of morphologically 300 distinct forms would appear to be unrealistically fast, especially given the known range of Th. cynocephalus is 301 nearly four million years (based on the late Pliocene age of the Chinchilla Local Fauna). Furthermore each of 302 these species can be diagnosed with autapomorphies, suggesting that none is an ancestor of any other)

Thus it would appear that for a brief period in the latest Miocene through to the earliest Pliocene the genus *Thylacinus* experienced a modest evolutionary radiation (Fig. 12). However the products of this radiation were short-lived and by the late Pliocene there is no indication of any surviving thylacinid species other on *Th. cynocephalus* (Dawson 1982). Unfortunately the Pliocene record of *Thylacinus* is sparse and scrappy (Mackness et al. 2002). Louys and Price (in press) report two specimens in the Queensland Museum that have been identified as *Th. rostralis* (=*Th. cynocephalus*) and genuinely derive from the Chinchilla Local Fauna. Apart from

303

304

305

306

307

310	(Mackness et al. 2002).
311	
312	Acknowledgemnts
313	I thank Ben McHenry of the South Australian Museum for access to the thylacinid specimens in his care. I also
314	thank Mary-Anne Binnie, also from the South Australian Museum, for organising a loan of material from that
315	institution. All photographs used in this paper, except figure 10 which was taken by the author, were taken by
316	Steven Jackson.
317	
318	References
319 320	Archer, M, Hand, S. J. and Godthelp, H., 1991. Riversleigh. The story of animals in ancient rainforests of inland Australia. Reed Books: Sydney. 264 pp.
321 322	Bonaparte C. L. J. L. 1838. Synopsis vertebratorium systematis. <i>Nuovi Annual, Science and Nature, Bologna</i> 2: 105-133.
323 324	Breed, W. and Ford, F. 2007. Native Mice and Rats. Australian natural history series. CSIRO Publishing: Collingwood. 185 pp.
325 326	Cohen, K.M., Finney, S.C., Gibbard, P.L. & Fan, JX. (2013) The ICS International Chronostratigraphic Chart. <i>Episodes</i> 36: 199-204.
327 328 329	Dawson, L. 1982. Taxonomic status of fossil thylacines (Thylacinus, Thylacinidae, Marsupialia) from late Quaternary deposits in Eastern Australia. Pp. 527-536, in Carnivorous Marsupials, (M. Archer. ed), Surrey Beatty and Sons and the Royal Zoological Society of New South Wales, Sydney.
330 331	Dickinson, J. A., Wallace, M. W., Holdgate, G. R., Gallagher, S.J. and Thomas, L. 2002. Origin and timing of the Miocene–Pliocene unconformity in southeast Australia. <i>Journal of Sedimentary Research</i> , 72: 288–303.
332 333	Fisher, D. O. and Blomberg, S. P. 2012. Inferring Extinction of Mammals from Sighting Records, Threats, and Biological Traits. Conservation Biology, 26: 57–67.
334 335	Gill T. 1872. Arrangement of the families of mammals with analytical tables. <i>Smithsonian Miscellaneous Collections</i> 2: 1–98.
336 337 338	Letnic, M., Fillios, M. and Crowther M. S. 2012. Could Direct Killing by Larger Dingoes Have Caused the Extinction of the Thylacine from Mainland Australia? <i>PLoS ONE</i> 7(5): e34877. doi:10.1371/journal.pone.0034877
339	Louys, J. and Price, G. J. In press. The Chinchilla Local Fauna: an exceptionally rich and well-preserved

- Pliocene vertebrate assemblage from fluviatile deposits of south-eastern Queensland, Australia. Acta
- 341 Palaeontologica Polonica. http://dx.doi.org/10.4202/app.00042.2013

342

- Mackness, B. S., Wroe, S., Wilkinson, C. and Wilkinson, D. 2002. Confirmation of *Thylacinus* from the Pliocene
- 344 Chinchilla Local Fauna. *Australian Mammalogy* 24: 237-241.
- Megirian D., Murray, P. and Wells, R. 1996. The Late Miocene Ongeva Local Fauna of central Australia. *The*
- 346 Beagle: Records of the Museums and Art Galleries of the Northern Territory 13: 9-38.
- 347 Megirian D, Prideaux GJ, Murray PF, Smit N. 2010. An Australian land mammal age biochronological scheme.
- 348 *Paleobiology* 36:658–671.

- 350 Murray PF. 1997. Thylacinus megiriani, a new species of thylacine (Marsupialia: Thylacinidae) from the Ongeva
- 351 Local Fauna of Central Australia. Records of the South Australian Museum 30: 43-61.
- 352 Murray PF, Megirian D. 2000. Two new genera and three new species of Thylacinidae (Marsupialia) from the
- 353 Miocene of the Northern Territory, Australia. The Beagle: Records of the Museums and Art Galleries of the
- 354 *Northern Territory* 16: 145-162.
- 355 Myers T. J. 2001. Prediction of marsupial body mass. *Australian Journal of Zoology* 49:99–118.
- 356 Paddle R. 2000. The last Tasmanian tiger: the history and extinction of the thylacine. Cambridge: Cambridge
- 357 University Press.
- 358 Pledge, N. S. 1992. The Curramulka Local Fauna: A new late Tertiary Fossil Assemblage from Yorke Peninsula,
- 359 South Australia. The Beagle: Records of the Museums and Art Galleries of the Northern Territory 9: 115-142.
- 360 Rich T. H. 1991. Monotremes, Placentals and Marsupials: their record in Australia and its biases. In Vertebrate
- Palaeontology of Australasia (Vickers-Rich, P, Monaghan, JM, Baird RF, Rich TH eds.) Pioneer Design Studio:
- 362 Melbourne 893-1070.
- 363 Swofford D. L. 2002. PAUP* phylogenetic analysis using parsimony (* and other methods). Version 4.
- 364 Sunderland, MA: Sinauer Associates.
- 365 Temminck, C. J., 1824. Monographies de Mammalogie. Tom. 1. Dufour: Paris. 60-65.
- 366 Thornback, J., and M. Jenkins. 1982. The IUCN mammal red data book, Part 1. International Union for
- 367 Conservation of Nature and Natural Resources, Gland, Switzerland.
- 368 Woodburne No. 1967. The Alcoota Fauna, central Australia. Bulletin of the Bureau of Mineral Resources
- 369 Geology and Geophysics, Australia 87: 1-187.
- Wroe S. 2001. Maximucinus muirheadae, gen. et sp. nov. (Thylacinidae: Marsupialia), from the Miocene of
- 371 Riversleigh, north–western Queensland, with estimates of body weights for fossil thylacinids. Australian
- 372 *Journal of Zoology* 49:603–614

373374375	Wroe, S. 2003. Australian marsupial carnivores: Recent advances in palaeontology. Pp. 102-123, in Predators with Pouches: The Biology of Marsupial Carnivores, (M. Jones, C. Dickman & M. Archer eds), CSIRO Publishing, Collingwood.
376377378	Wroe, S. and Muirhead, J. 1999. Evolution of Australia's marsupicarnivores: Dasyuridae, Thylacinidae, Myrmecobiidae, Dasyuromorphia <i>incertae sedis</i> and Marsupialia <i>incertae sedis</i> . <i>Australian Mammalogy</i> 21: 10.11.
379 380 381	Yates, A M. 2014. New craniodental remains of <i>Thylacinus potens</i> (Dasyuromorphia: Thylacinidae), a carnivorous marsupial from the late Miocene Alcoota Local Fauna of central Australia. <i>PeerJ</i> 2:e547; DOI 10.7717/peerj.547
382	
383	Appendix 1. Character-Taxon Matrix
384	The character list is provided in Yates (2014).
385	Barinya wangala
386	0?000010000000000001000000000000000
387	Antechinus flavipes
388	000001000000000000000000000000000000000
389	Muribacinus gadiyuli
390	01??????10000000000000001000?1000000000
391	Badjcinus turnbulli
392	00?01000?00?0?000000??100000001?2010100010
393394	Mutpuracinus archibaldi 0 ? 0 ? 0 0 0 0 1 0 0 0 0 0 0 0 0 0 0 0
394	Nimbacinus dicksoni
396	0001100010001?000000??010?0001??101000000
397	Nimbacinus richi
398	?00??000100010?00010000111?101000?000
399	Maximucinus muirheadae
400	??????????10?0200????10?????????????
401	Ngamalacinus timmulvaneyi
402	?1???1001?00??0?0000?10????1011100010
403	Wabulacinus ridei
404	00???????1?11?021111??10111??01??11001?1?0
405	Tyarrpecinus rothi
406	?????011?10010110101??000?00???????????
407	Thylacinus macknessi
408	????????0?11?02??10??10????01102111010110
409	Thylacinus potens

410 ??1??0111001?0122210001?100010002221011102

411	Thylacinus megiriani
412	111??001?21?001?221111111001?111?221?1??02
413	Thylacinus cynocephalus
414	210111000211111222111110121101112221011101
415	Thylacinus yorkellus
416	????????????????????????0111222101?1?1
417	
418	

1

Thylacinus yorkellus, holotype SAM P29807, incomplete left dentary.

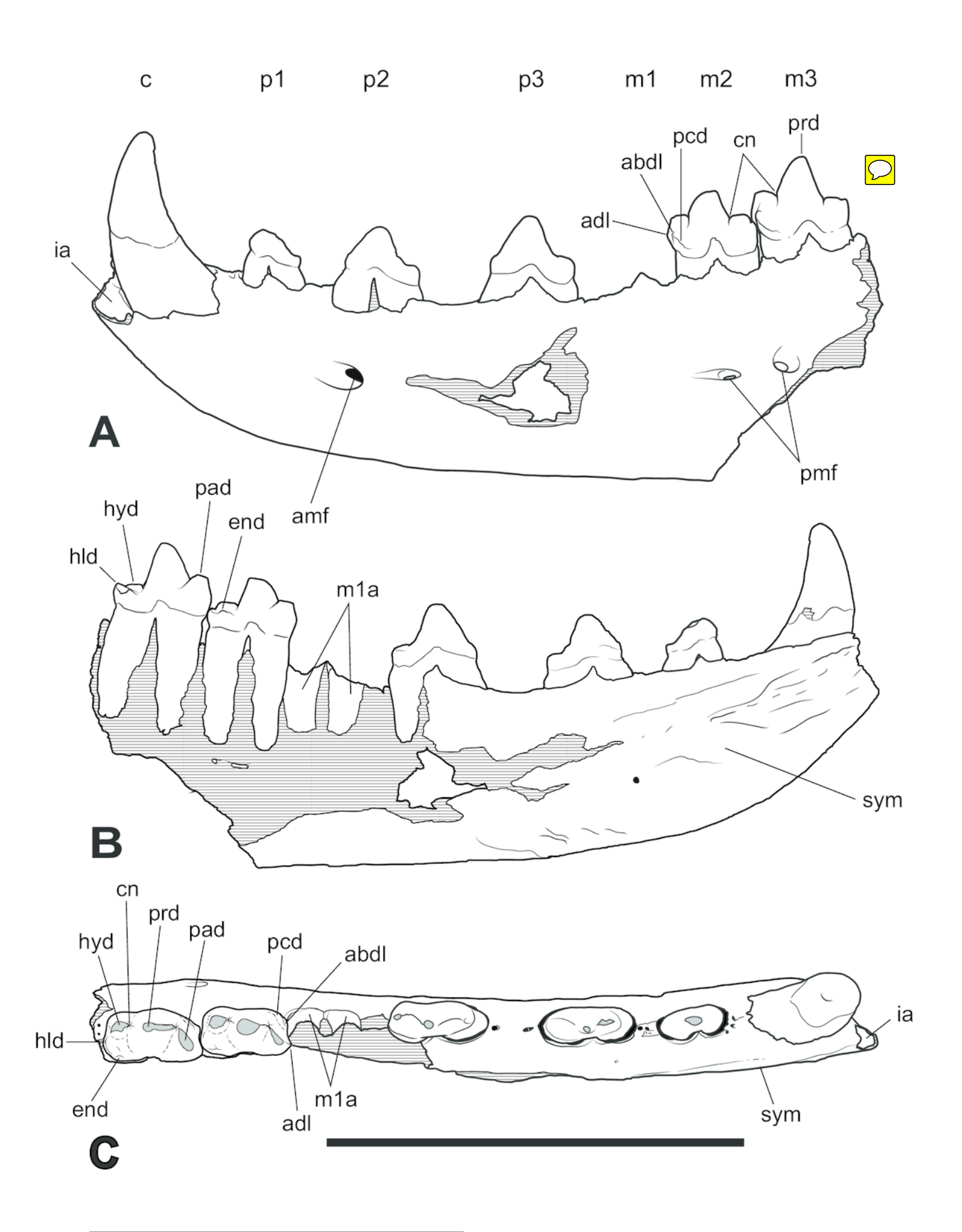
Photographs of the specimen. (A) lateral view. (B) medial view. (C) dorsal view. Scale bar = 50 mm.



2

Thylacinus yorkellus holotype SAM P29807, incomplete left dentary.

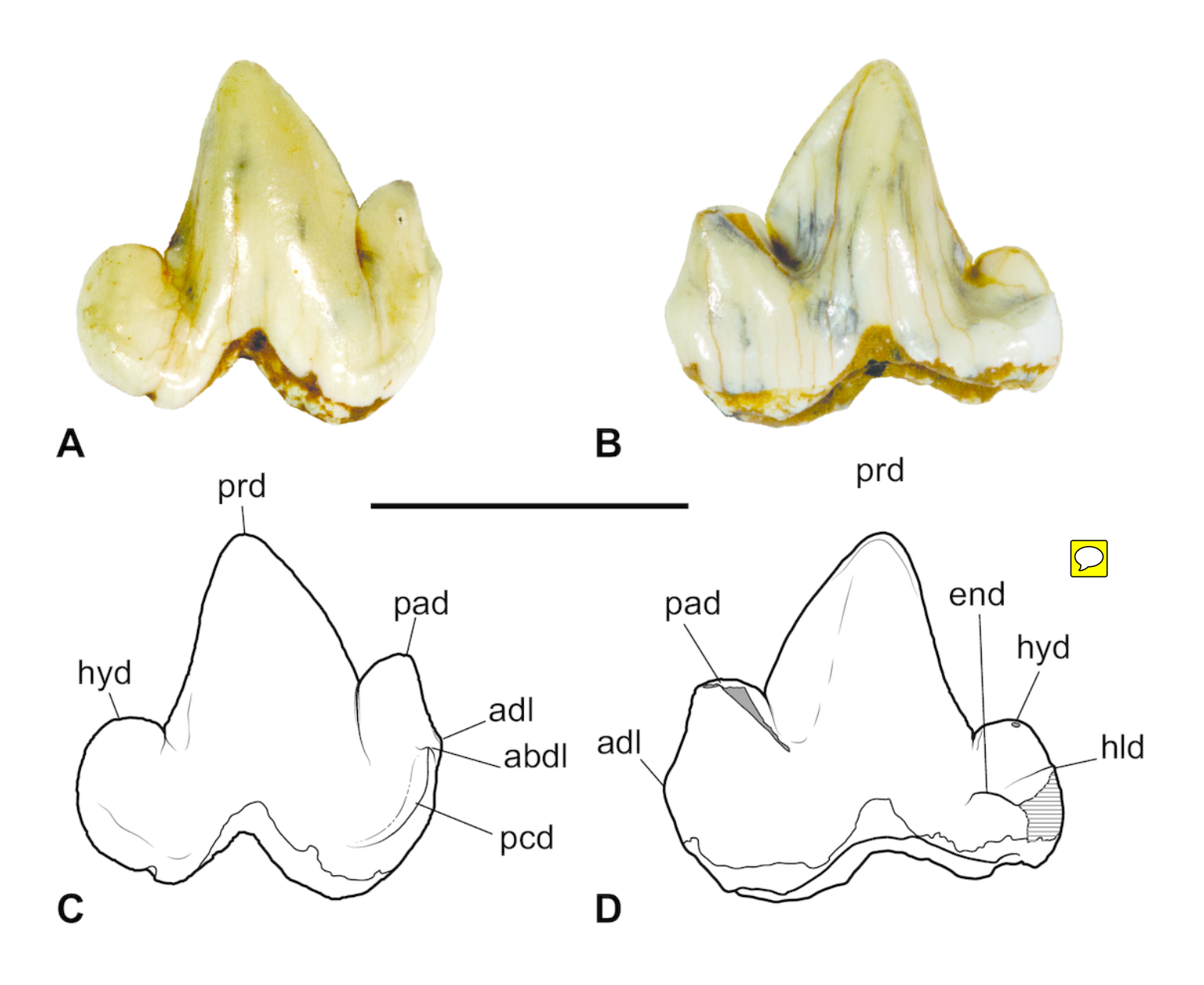
Interpretive drawings of the specimen. (A) lateral view. (B) medial view. (C) dorsal view. Abbreviations: adl, anterior cuspidule; abdl, anterobuccal cuspidule; amf, anterior mental foramen; c, canine; cn, carnassial notch; end, entoconid; hld, hypoconulid; hyd, hypoconid; ia, incisor alveoli; m1-3, molars 1-3; p1-3, premolars 1-3; pad, paraconid; pcd, precingulid; pmf, posterior mental foramen; prd, protoconid; sym, symphyseal surface. Hatched areas represent broken bone surfaces, grey areas represent wear facets on the teeth. Scale bar = 50 mm.



3

Thylacinus yorkellus, paratype SAM P38799, right m_{3.}

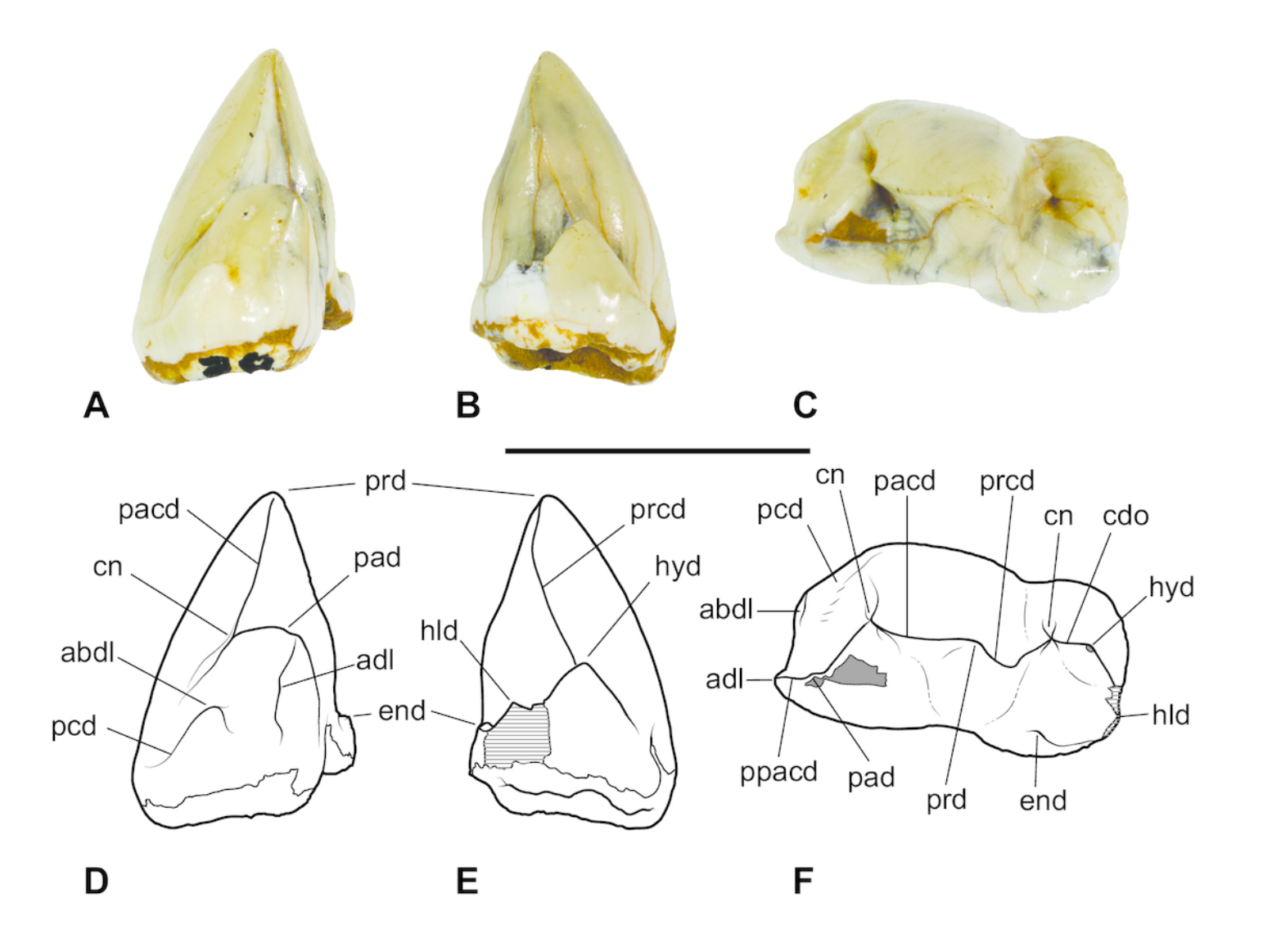
- (A) photograph in buccal view. (B) photograph in lingualview. (C) Interpretive drawing of A.
- (D) Interpretive drawing of B.Abbreviations: adl, anterior cuspidule; abdl, anterobuccal cuspidule; cn,carnassial notch; end, entoconid; hld, hypoconulid; hyd, hypoconid; pad,paraconid; pcd, precingulid; prd, protoconid; Scale bar = 10 mm. [p]



4

Thylacinus yorkellus, paratype SAM P38799, right m₃

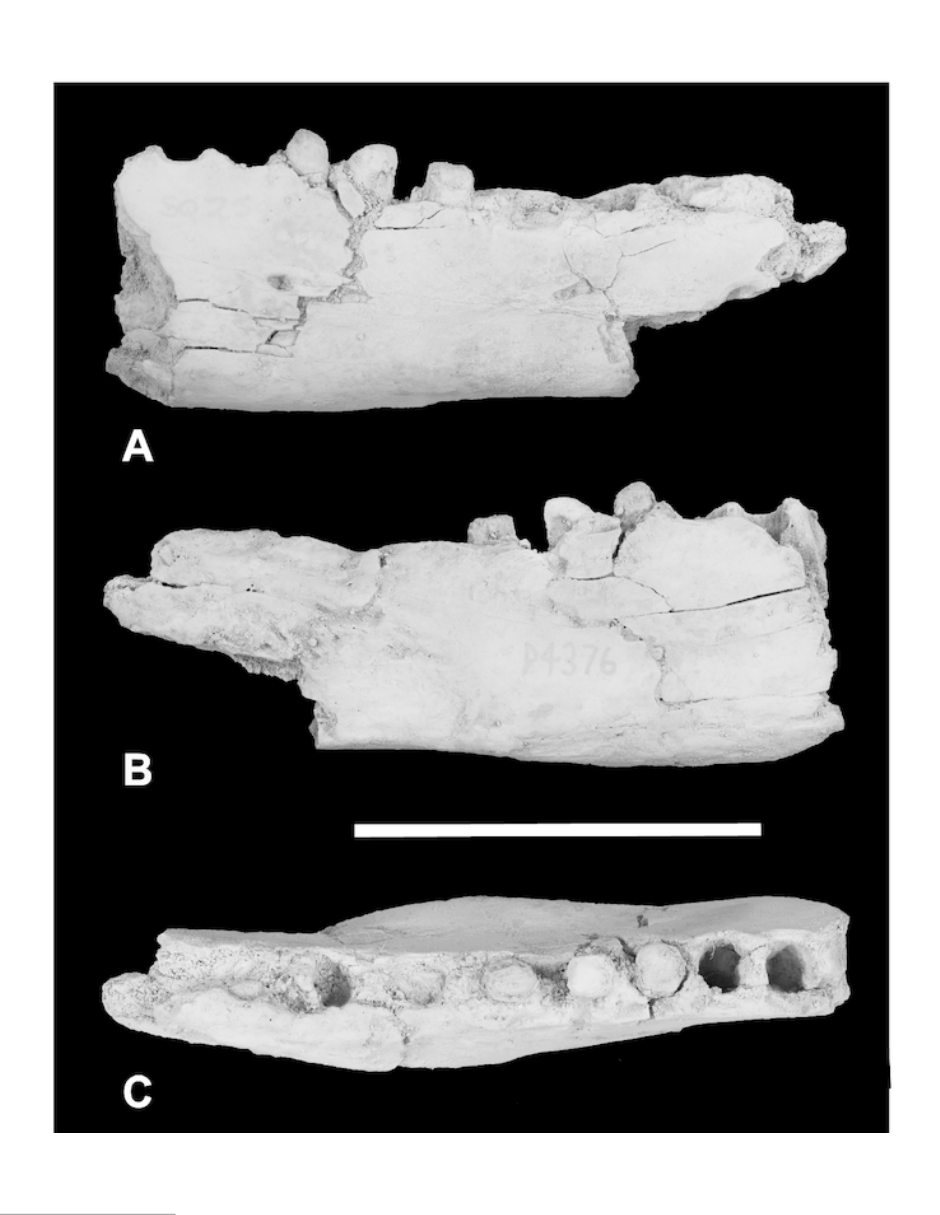
(A) photograph in anterior view. (B) photograph in posterior view. (C) photograph in occlusal view (D) Interpretive drawing of A. (E) Interpretive drawing of B (F) Interpretive drawing of C. Abbreviations: adl, anterior cuspidule; abdl, anterobuccal cuspidule; cdo, cristid obliqua; cn, carnassial notch; end, entoconid; hld, hypoconulid; hyd, hypoconid; pacd, paracristid; pad, paraconid; pcd, precingulid; ppacd, preparacristid; prcd, protocristid; prd, protoconid; Scale bar = 10 mm.



5

Thylacinus megiriani, NTM P4376, fragmentary right dentary.

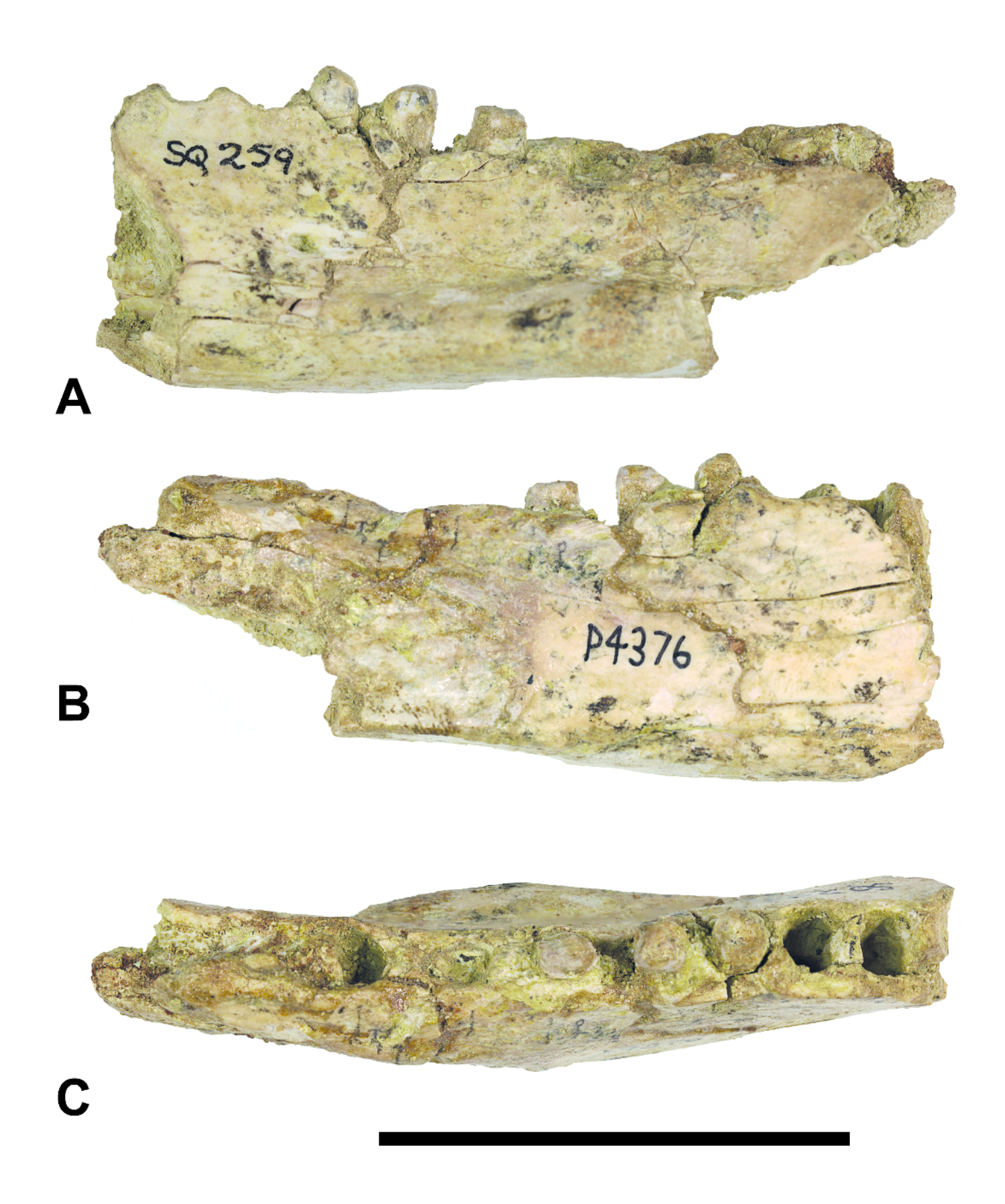
Monochrome photographs of the specimen after whitening with ammonium chloride. (A) lateral view. (B) medial view. (C) dorsal view. Scale bar = 50 mm.



6

Thylacinus megiriani, NTM P4376, fragmentary right dentary.

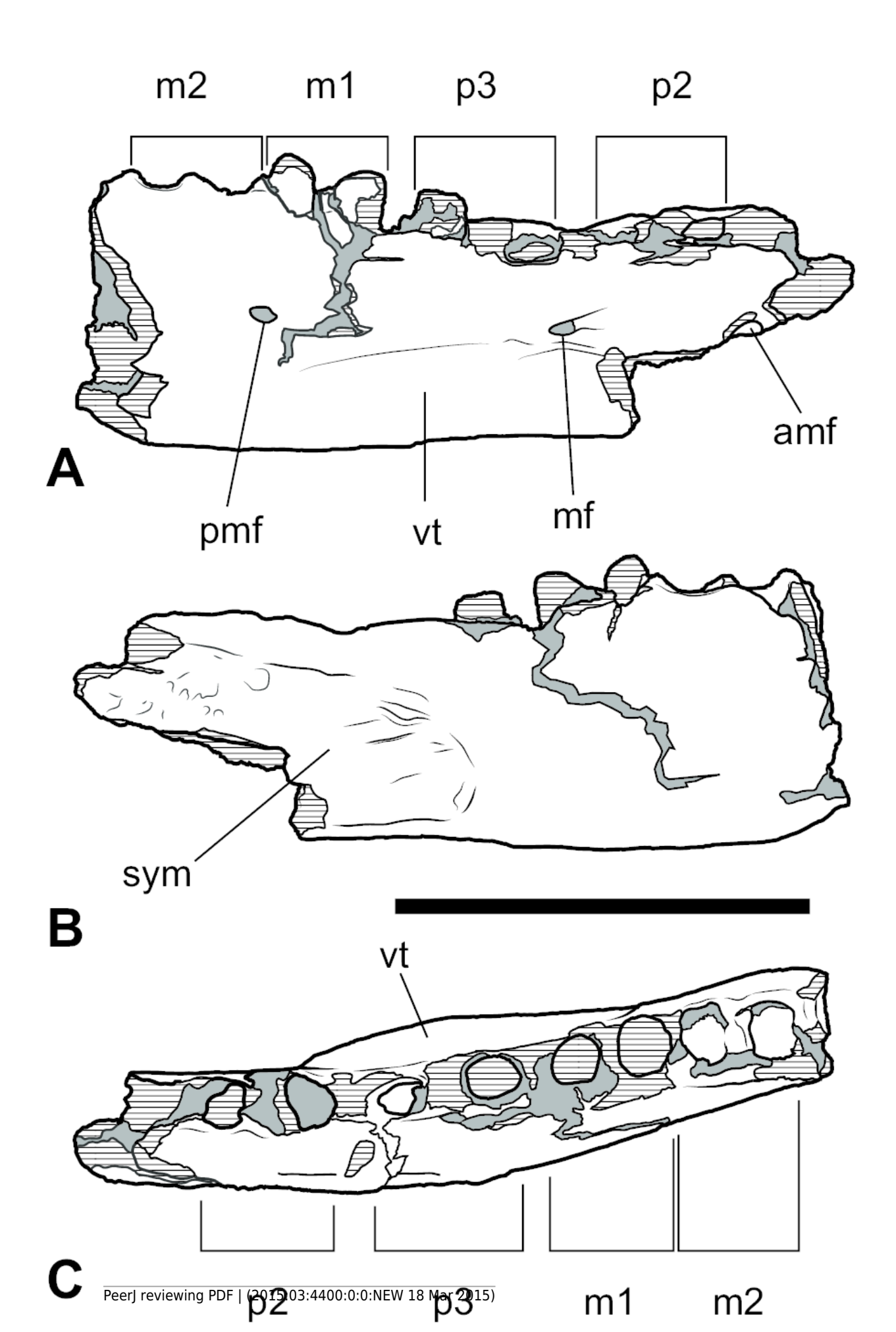
Colour photographs of the specimen. (A) lateral view. (B) medial view. (C) dorsal view. Scale bar = 50 mm.



7

Thylacinus megiriani, NTM P4376, fragmentary right dentary.

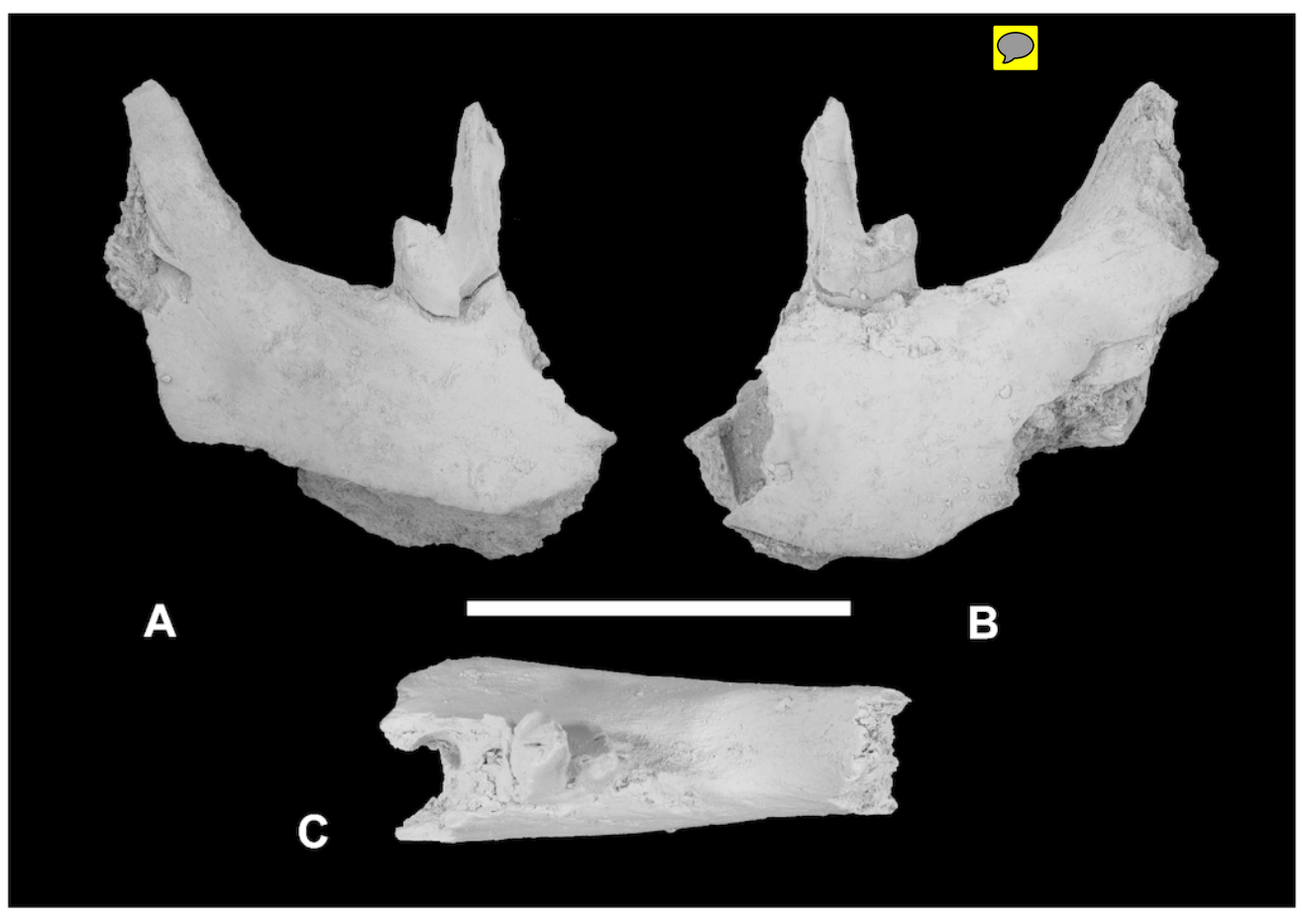
Interpretive drawings of the specimen. (A) lateral view. (B) medial view. (C) dorsal view. Abbreviations: amf, anterior mental foramen; m1-2, molars 1-2; mf, mental foramen; p1-2, premolars 1-2; pmf, posterior mental foramen; sym, symphyseal surface; vt, ventral torus. Hatched areas represent broken bone surfaces, grey areas represent patches of matrix. Scale bar = 50 mm.

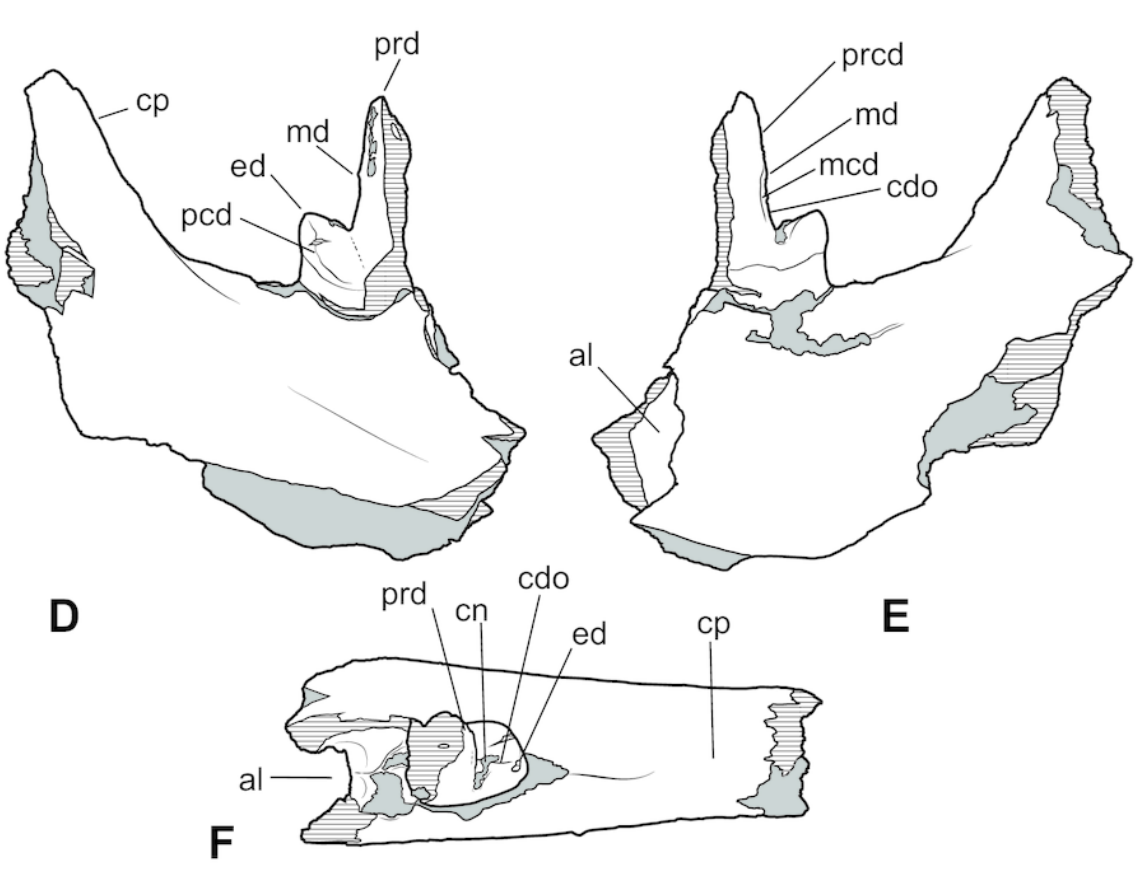


8

Thylacinus megiriani, NTMP4377, fragment of right dentary including partial right m4.

(A-C) monochrome photographs of the specimen after whitening with ammonium chloride. (D-F) interpretive drawings of A-C. (A, D) lateral view. (B, E) medial view. (C, F) dorsal view. Abbreviations: al, alveolus for anterior root of m4; cdo, cristid obliqua; cn, carnassial notch; cp, base of coronoid process; ed, entoconid; mcd, metacristid; md, metaconid; pcd, postcristid; prcd, protocristid; prd, protoconid. Grey areas represent patches of matrix, hatched areas represent broken bone or tooth surfaces. Scale bar = 30 mm.





9

Thylacinus megiriani, NTMP4377, fragment of right dentary including partial right m4.

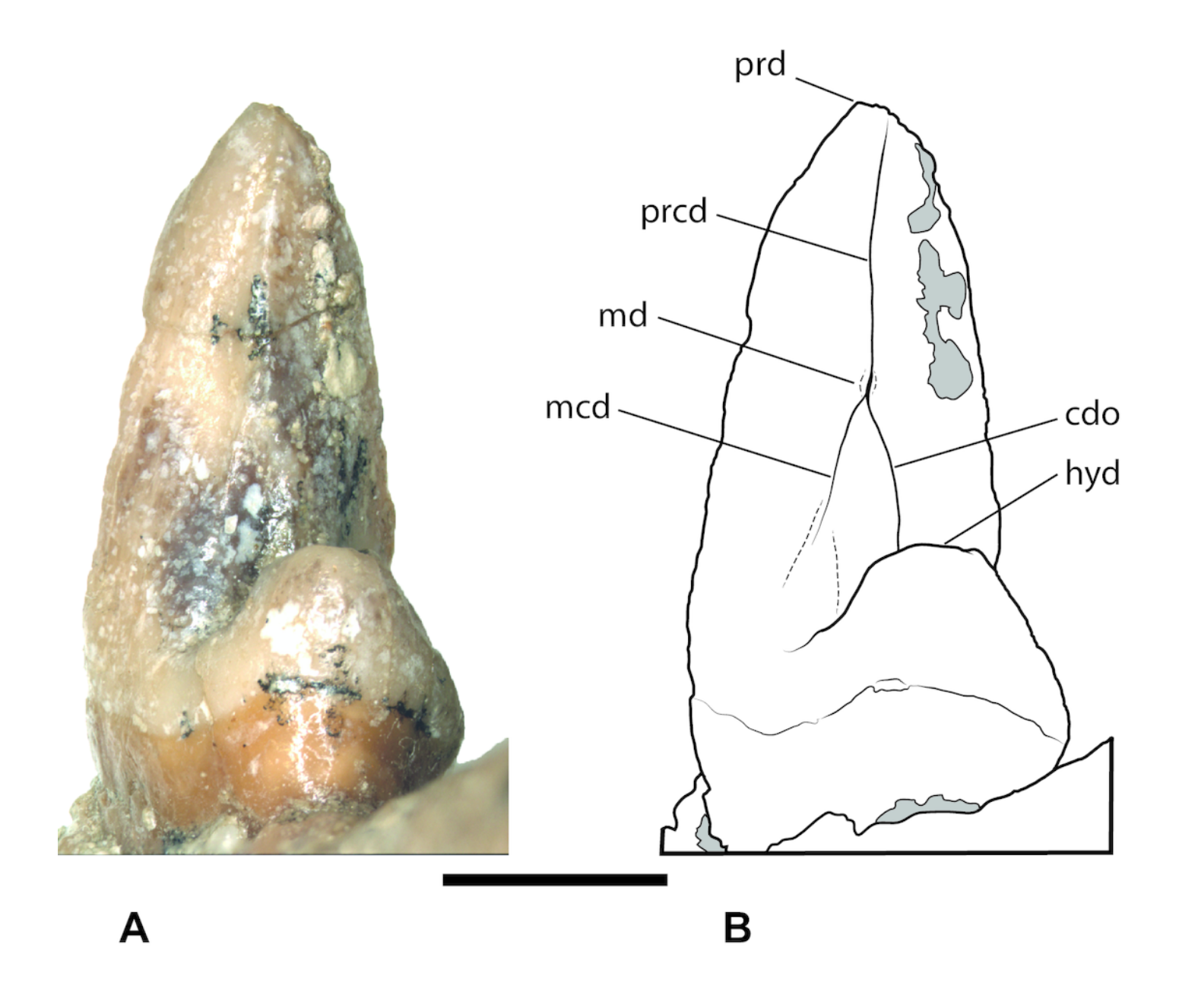
Colour photographs of the specimen. (A) lateral view. (B) medial view. Scale bar = 30 mm.



10

Thylacinus megiriani, NTM P4377, right m₄ in posterolingual view.

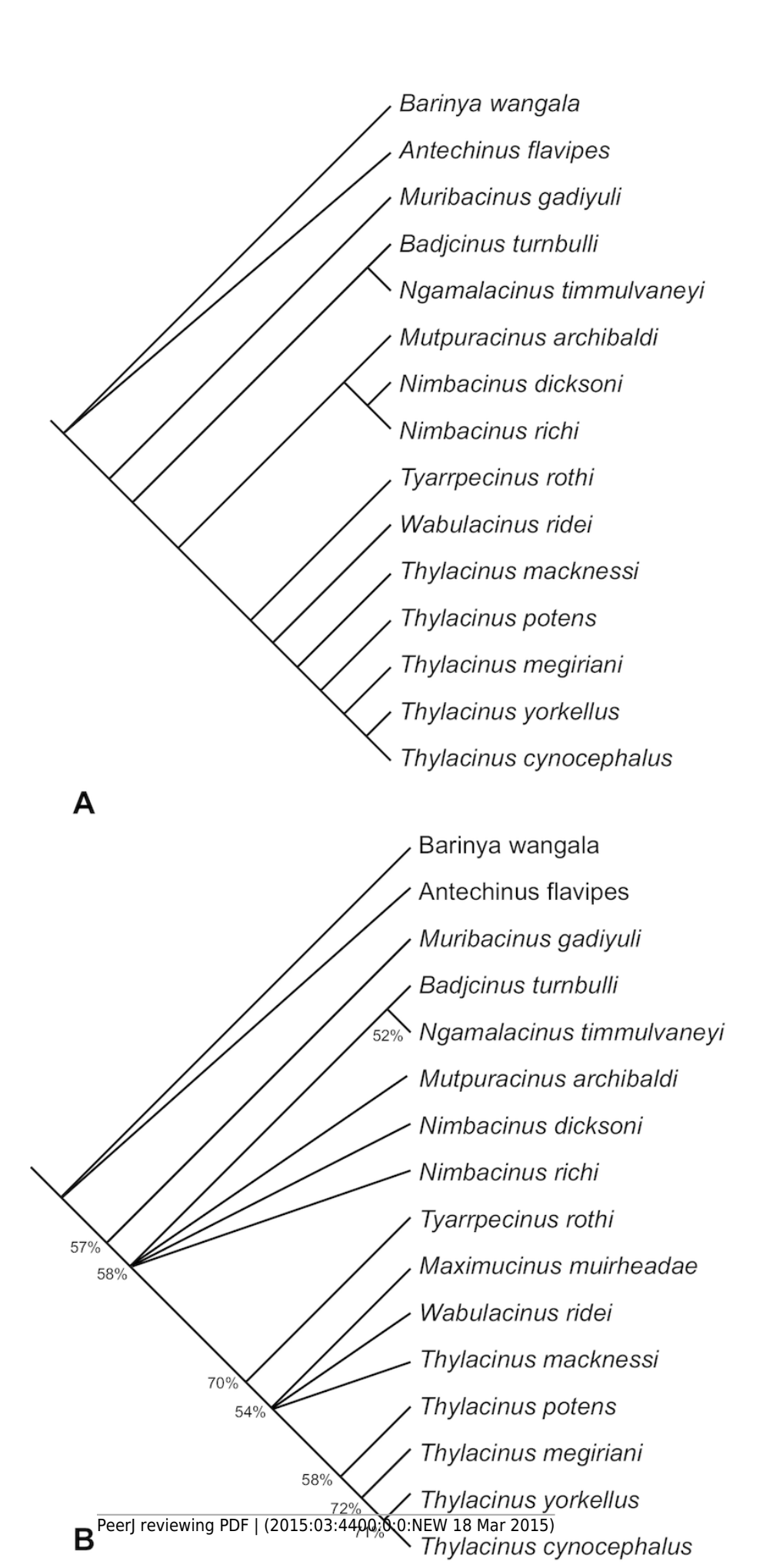
(A) photograph. (B) interpretive drawing. Abbreviations: cdo, cristid obliqua; hyd, hypoconid; mcd, metacristid; md, metaconid; prcd, protocristid; prd, protoconid. Grey areas represent patches of adherent matrix. Scale bar = 5 mm.



11

Results of the cladistic analysis of thylacinid interrelationships.

A) reduced cladistic consensus tree of two most parsimonious trees (tree length = 93 steps) obtained after a posteriori pruning of *Maximucinus muirheadae*. (B) strict consensus with bootstrap support values for clades with values > 50 %.



12

A phylogenetic tree of *Thylacinus*, calibrated to the geological timescale.

Note that the dates of *Th. potens, Th. megiriani* and *Th. yorkellus* are not tightly constrained and the ages given here are approximations with the grey bars indicating a range of plausible ages. Numbers represent ages in ma. Dates of boundaries taken from Cohen et al. (2013).

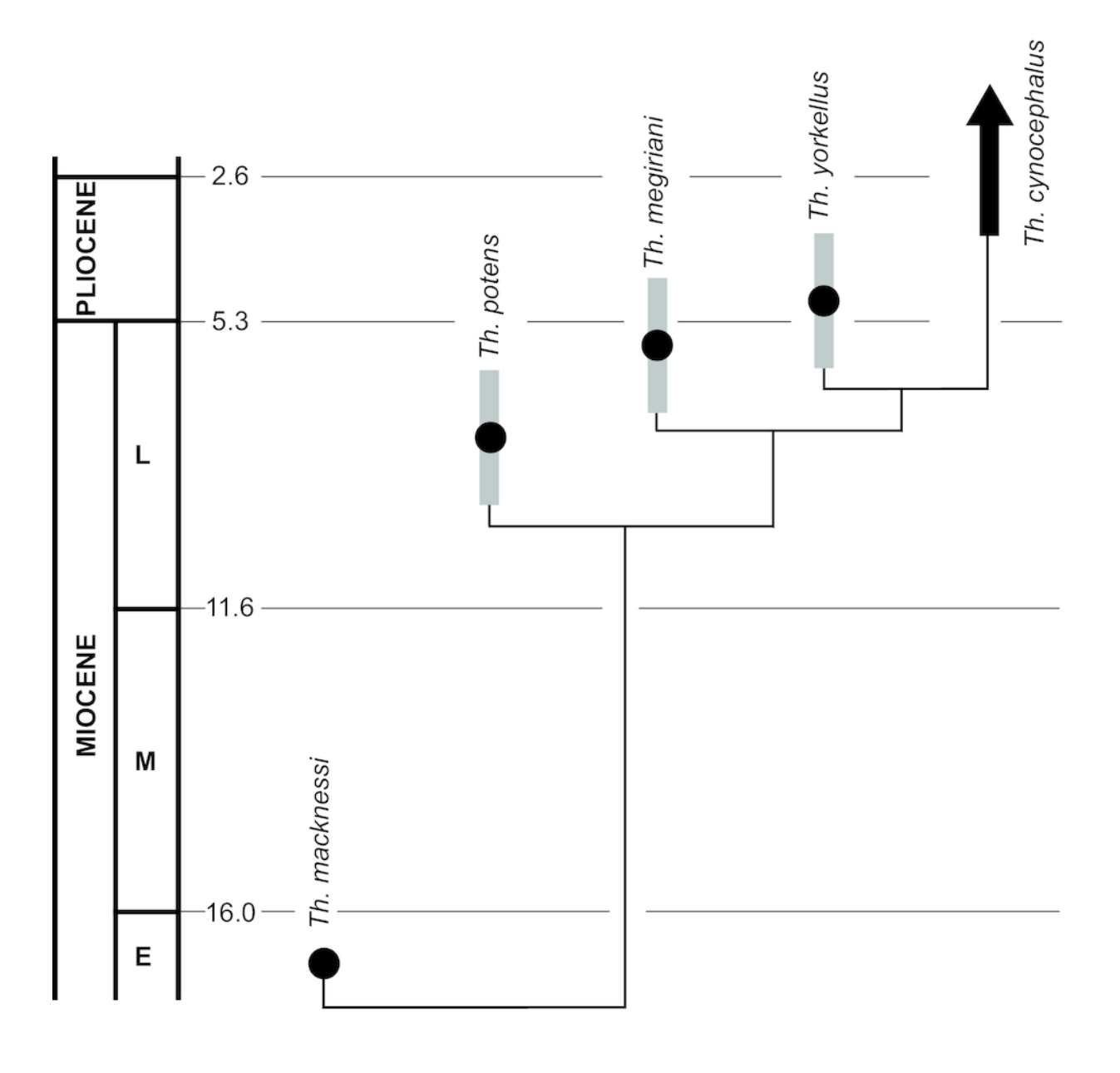


Table 1(on next page)

Canine measurements of *Thylacinus yorkellus*.

Holotype SAM P29807.

Height (mm)	Basal Length (mm)	Basal Width (mm)
15.2	8.7	6.5

Table 2(on next page)

Dental measurements of *Thylacinus yorkellus*.

Abbreviations: L, anteroposterior length of the crown; W, maximum buccolingual width of the crown; trigW, buccolingual width of the trigonid; talW, buccolingual width of the talonid.

Measurements are in mm. Note that M1L of SAM P29807 is an approximation based on the measurement taken from the empty alveolus.

	P ₁ L	P ₁ W	P ₂ L	P ₂ W	P ₃ L	P ₃ W	M ₁ L	M ₂ L	M ₂ trigW	M ₂ talW	M ₃ L	M ₃ trigW	M ₃ talW
SAM P29807	7.2	3.1	9.8	4.0	10.4	4.4	~8.7	11.0	5.5	5.8	12.0	6.5	5.7
SAM P38799	-	-	-	-	-	-	-	-	-	-	11.3	6.0	6.0

Table 3(on next page)

Approximate basal lengths of the teeth in *Thylacinus megiriani*.

Referred specimen, NTM P4376. Measurements taken from alveoli.

P ₂ (mm)	P ₃ (mm)	M ₁ (mm)	M ₂ (mm)
15.6	18.0	14.3	13.4

Table 4(on next page)

Dental measurements of *Thylacinus megiriani*.

Referred specimen, NTM P4377. Abbreviations: H, height of crown, from crown-root junction to tip of protoconid; trigW, buccolingual width of trigonid; talW, buccolingual width of talonid. Note that trigonid width is measured as preserved and that due to incompleteness this represents a minimum value and that the true value may have been greater.

M₄H (mm)	M₄trigW (mm)	M₄talW (mm)
16.9	(7.3)	6.5